Evidence of a long-range density gradient in SiO_2 films on Si from H_2-permeability measurements

B. J. Mrstik
Code 6816, Naval Research Laboratory, Washington, D.C. 20375

P. J. McMarr
SFA, Inc., Landover, Maryland 20785

(Received 28 June 1993)

We describe a technique for the measurement of the diffusivity, solubility, and permeability of H_2 through SiO_2 thermally grown on Si substrates at room temperature. We have applied this technique to determine the dependence of the H_2 permeability on oxide thickness and growth temperature. Since permeability depends strongly on density, these measurements provide a sensitive probe of the oxide density. Our results indicate that the H_2 permeability is considerably less in SiO_2 films thermally grown on Si substrates than through bulk SiO_2, in agreement with previous works which had indicated that thermally grown oxides are denser than bulk SiO_2. The permeability is found to decrease with oxide thickness, indicating that thinner oxides have larger densities than thicker oxides. Oxides grown at high temperatures are found to have higher permeabilities than oxides of similar thickness grown at lower temperatures. We present evidence that the dependence of permeability on oxide thickness results from a density gradient throughout the oxide rather than from a uniform reduction of the oxide density as the oxide becomes thicker.

I. INTRODUCTION

Because the operation of silicon metal-oxide-semiconductor (MOS) devices depends strongly on the properties of the thermal oxide and of the Si-SiO_2 interface, there have been numerous studies of the structure of the oxide, especially near the interface. Although some theoretical work[1] had indicated that an abrupt interface was geometrically and energetically favorable (at 0 K), most early experimental results using a wide variety of techniques indicated that the interfacial region had a small surplus of Si. The experimental situation as of 1980 is summarized in Ref. 2. One of the first investigations to determine both the width *and* the stoichiometry of the interfacial region was the spectroscopic ellipsometry study of Aspnes and Theeten[2] which reported that an oxide grown in dry oxygen at 1000 °C had a transition layer with a thickness of 7±2 Å and a stoichiometry of SiO_x where $x=0.4\pm0.2$. In this analysis it was assumed that the bulk of the oxide had a uniform density.

Grunthaner and co-workers used x-ray photoemission spectroscopy (XPS) and chemical etching to characterize the Si-SiO_2 interface of oxides grown in dry oxygen at 1000 °C. Their work[3] describes the interface as having a layer approximately 5 Å thick at the Si interface which is composed of a mixture of various silicon suboxides. There is also a region of stoichiometric strained SiO_2 approximately 15–30 Å wide in which the density of the oxide changes from approximately that of the SiO_x layer (which they estimate to be 3.8 g/cm^3) to that of unstrained SiO_2 (2.20 g/cm^3). This density change is achieved by gradually increasing the SiO_2 ring size.

It is well known that the refractive indexes of thermally grown oxides depend on their growth temperature, with oxides grown at lower temperatures having larger indexes. Although this is a strong indication that thermal oxides differ from bulk SiO_2, there is little consensus about the actual oxide structure. As discussed in Sec. IV, some work[4] indicates that the oxide becomes optically identical to bulk SiO_2 at a distance of about 60 Å from the interface, whereas other work[5] indicates that the oxide further than 7 Å from the interface has a uniform refractive index which is greater than that of bulk SiO_2.

We have studied the structure of thin thermally grown SiO_2 films on Si substrates by measuring their permeability to hydrogen gas. Since permeability is extremely sensitive to density, these measurements provide an excellent probe of the oxide density. We have used this probe to study pyrogenic and dry oxides. Our results indicate that the oxides have a density gradient which extends at least several hundred Å from the interface. We show how these results are in general agreement with the results of several other studies.

II. METHOD FOR DETERMINATION OF PERMEABILITY

A. Introduction

There are several standard methods for determining the solubility S, diffusivity D, and permeability $K\equiv SD$ of a gas through bulk specimens.[6] One technique involves exposing one side of a membrane of the material to the gas and measuring the rate at which the gas evolves from the other side. In another type of measurement the material is saturated with the gas, then the evolution of gas from the sample is monitored during degassing. Since such techniques cannot be applied to the measurement of

0163-1829/93/48(24)/17972(14)/$06.00 ©1993 The American Physical Society

gas permeability through a thin film in contact with a substrate, another method must be devised.

Thermally grown oxide films are formed by diffusion of the oxidant (either O_2 or H_2O) through the oxide. The rate at which the oxide grows therefore depends on the permeability of the oxidant, and has been modeled by Deal and Grove.[7] For thick oxides, the H_2O and O_2 permeabilities estimated by fitting the model parameters to experimental growth rate data are in good agreement with the values determined from studies of diffusion through bulk SiO_2.[8,9] But for thin oxides grown in dry oxygen the Deal-Grove growth rate model is in poor agreement with experimental data, and cannot be used to determine the O_2 permeability.

The transport of hydrogen through thermally grown films of SiO_2 on Si has been studied in at least two previous works.[10,11] In both studies passivation of interface traps in metal-oxide-semiconductor (MOS) capacitors by hydrogen was used to determine the hydrogen diffusivity. Schols and Maes[10] observed the spatial variation in the number of interface traps (N_{it}) as hydrogen diffused laterally across a MOS capacitor at 700–1000 °C. They observed a sharp boundary between regions of low and high N_{it}, and estimated the H_2 diffusivity by measuring the velocity at which this boundary moved across the capacitor. They did not consider the effect of H_2 consumption at the interface on the velocity of the front, however. As we will show later, consumption of H_2 can significantly affect the rate at which the H_2 appears to be diffusing.

Fishbein, Watt, and Plummer[11] made a similar study at temperatures from 400 °C to 500 °C. They included the effect of H_2 consumption by developing a model for the chemistry of interface trap passivation. The values of the H_2 diffusivity obtained by fitting this model to their experimental data are within a factor of 2 of those reported in Ref. 10 when extrapolated to the higher temperature range. Significantly, the diffusivities reported in both of these studies were almost two orders of magnitude smaller than the results reported for bulk SiO_2.[12–14]

Since the techniques used in Refs. 10 and 11 depend on the passivation of interface traps by H_2, they can only be used at temperatures above about 225 °C at which appreciable passivation occurs.[15] An earlier publication[16] outlined a method for determining the room temperature permeability of H_2 through SiO_2 films on Si, and applied the method to study the permeability of pyrogenic oxides. The value obtained for K was only approximate, however, since it depended (weakly) on the value of S, which could not be accurately determined. In this paper we show how this technique can be enhanced to obtain accurate values for both S and D independently, so that a more accurate value of K can be obtained. The method has been applied to determine the thickness dependence of the permeability of both dry and pyrogenic oxides.

The technique used for the determination of K is based on an earlier observation[17] that x-ray irradiation of SiO_2 forms defects in the oxide which are able to crack H_2 molecules introduced into the oxide at room temperature after irradiation. As a result of the cracking of the hydrogen molecules, the number of traps at the Si-SiO_2 interface (N_{it}) increases during the hydrogen exposure and the number of traps in the bulk of the oxide (N_{ot}) decreases. A short description of this effect will be presented in Sec. II C. The details of how this effect has been utilized to determine the permeability of H_2 in SiO_2 films on Si substrates will then be presented in Sec. II D. The next section will describe the preparation of the samples used in these studies, and the techniques used to measure N_{it} and N_{ot}.

B. Sample preparation and measurement of N_{it}

Samples used for the permeability measurements were MOS field effect transistors (MOSFET) fabricated on (100) Si substrates. The standard LOCOS (location oxidation of silicon) method was used for isolation. The gate electrodes were 5000 Å thick films of polysilicon. All devices received a postmetallization anneal in forming gas at 400 °C. Most of the MOSFET's had gate oxides which were grown at 900 °C and had p-type channels. The gate oxides of one subset of these samples were grown in dry oxygen and those of another subset were grown in a mixture of hydrogen and oxygen (pyrogenic oxides). The pyrogenic oxidations were preceded and followed by a 5-min dry oxidation. The oxides were grown to various thicknesses ranging from 95 to 1140 Å. In addition, some of the pyrogenic oxides were prepared by first growing the oxide to 1082 Å, then etching back to form a thinner oxide. One group of the pyrogenic oxides were annealed in 33% H_2 at 900 °C for 1 h. Another set of MOSFET's had gate oxides which were grown at 1000 °C in dry oxygen to a thickness of 772 Å, and had n-type channels. A summary of the samples used for the permeability measurements is shown in Table I.

A different set of samples was used in the preliminary studies of hydrogen cracking discussed in Sec. II C. These samples were prepared similarly, but were n-channel MOSFET's whose gate oxides were grown in dry oxygen at 900 °C on (100) Si to a thickness of 770 Å or on (111) Si to a thickness of 557 Å. The effects of hydrogen exposure on N_{it} described in Sec. II C were similar for all the samples.

A side view of the MOSFET's is shown in Fig. 1. Several MOSFET's are fabricated on each chip. All MOSFET's on the same chip have identical gate oxide thicknesses T, and gate widths W (≈ 140 μm), but have different gate lengths L_g, varying from about 2 to 23 μm. An important feature of these MOSFET's is that the gate oxide is exposed to the ambient along the width of the device so that gas from the ambient can enter the gate along these two sides of the gate oxide, then diffuse the length of the gate oxide. Each chip is mounted in its own ceramic package, so that all devices on the chip are exposed to the same irradiation and ambient gas. The gate width and gate length of each MOSFET were measured at the end of the experiment using an electron microscope. The gate oxide thicknesses were determined from single wavelength ellipsometry measurements on dummy wafers prepared at the same time as the device wafers.

The samples were x-ray irradiated in air at room tem-

TABLE I. Summary of gate oxides studied. Substrates for all oxides were (100) silicon.

Oxide thickness (Å)	Dry or pyrogenic[a] oxide	Growth temperature (°C)	Channel type	Notes
1082	pyrogenic	900	p	
478	pyrogenic	900	p	Annealed in 33% H_2 for 1 h at 900 °C prior to device fabrication
457	pyrogenic	900	p	Etched back from 1082 Å
354	pyrogenic	900	p	
236	pyrogenic	900	p	
214	pyrogenic	900	p	Etched back from 1082 Å
161	pyrogenic	900	p	Etched back from 1082 Å
1140	dry	900	p	
422	dry	900	p	
146	dry	900	p	
95	dry	900	p	
772	dry	1000	n	

[a]Pyrogenic oxidation was preceded and followed by a 5-min dry oxidation.

perature using a 10 keV ARACOR system with a tungsten target tube. Various x-ray doses from 0.1 Mrad to 10 Mrad were used. The dose rate was always 1.8 (SiO_2) krad/sec. During the irradiations the gate electrodes were held at a positive bias to maintain a field across the oxide of 1 MV/cm. This gate bias was maintained for approximately 24 h after irradiation before exposing the MOSFET's to hydrogen at room temperature. The hydrogen was in the form of either pure H_2 or forming gas (10.0% H_2 and 90.0% N_2). The gate bias was maintained at the same value during hydrogen exposure as during irradiation.

Measurements of N_{it} were made using charge pumping techniques as described by Grosenecken *et al.*[18] In this technique the source and drain of the MOSFET are connected together and held at a small reverse bias relative to the substrate. A trapezoidal shaped voltage pulse is applied to the gate electrode with a frequency ω. The upper and lower limits of the pulse are chosen so as to move the Si surface between inversion and accumulation. The resulting current flowing from the source and drain into the substrate is measured. This charge pumping current, I_{cp}, is the recombination current flowing through the interface traps, and is given by

$$I_{cp} = q\omega A N_{it} \ , \tag{1}$$

where q is the electronic charge, and A is the area of the Si surface being pumped. N_{it} is the number of traps in a limited region about the center of the band gap. The extent of the band gap being probed depends on the rise and fall times of the trapezoidal pulse applied to the gate. By varying the rise and fall times, therefore, the spectral distribution of the number of interface traps in the band gap, D_{it}, may be determined.[18] In the measurements of D_{it} reported here the pulse rise and fall times were varied from 1.25×10^{-8} sec to 1.25×10^{-2} sec, so that D_{it} was measured as a function of energy from approximately 0.16 to 0.94 eV above the conduction band edge. For the measurements of N_{it} a pulse with a frequency of 62.5 kHz and rise and fall times of 4 μsec was used, so that the number of interface traps in approximately the central 0.5 eV of the band gap was measured.

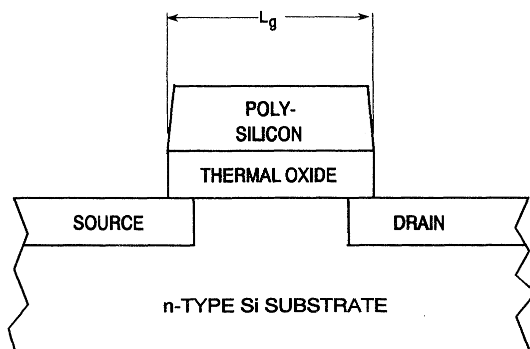

FIG. 1. Side view of MOSFET structure. Device has no passivating layer, so the thermal oxide is exposed to ambient.

C. Experimental background

Figure 2 shows D_{it} after irradiation for a representative MOSFET before hydrogen exposure and after a long exposure. Before irradiation D_{it} is approximately two orders of magnitude smaller than the values shown in Fig. 2. The hydrogen exposure results in approximately a factor of 2 increase in the number of interface traps in the band gap. As Fig. 2 indicates, however, the energy *distri-*

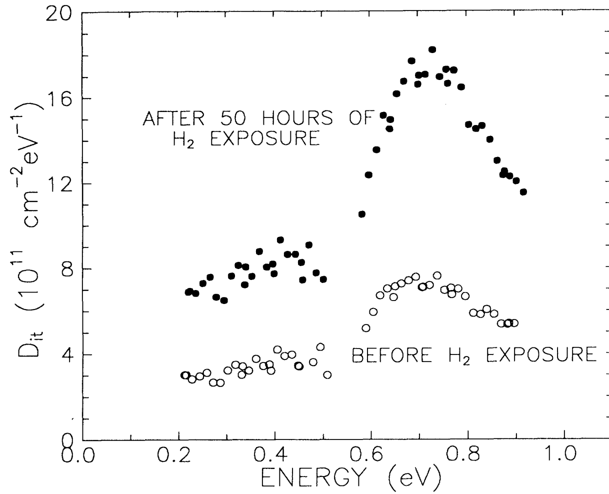

FIG. 2. Density of interface traps (D_{it}) as function of energy above valence band edge. Values before hydrogen exposure and after 550 h exposure to forming gas (10.0% H_2) are shown. Data were obtained on a MOSFET with a 354 Å dry oxide grown at 900 °C. The MOSFET had been irradiated with x rays to a dose of 2.0 Mrad.

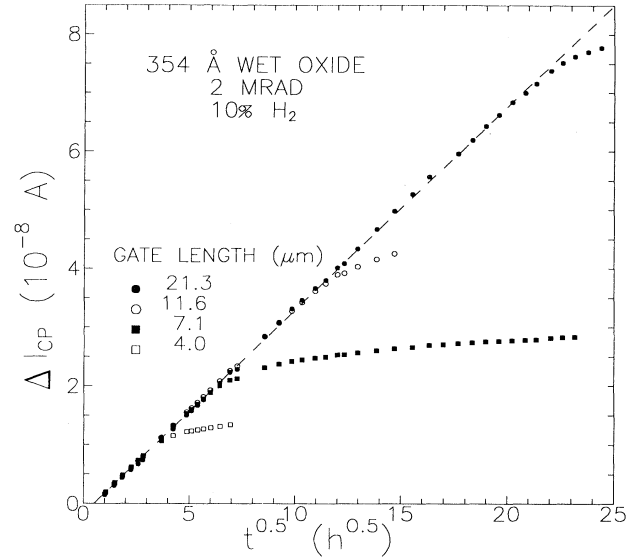

FIG. 3. Change in charge pumping current (I_{cp}) as a function of square root of time in hours. Data for four MOSFET's on a single chip are shown. MOSFET's are identical except for their gate lengths. Devices were simultaneously irradiated to a dose of 2.0 Mrad of x rays, then exposed to forming gas (10.0% H_2).

bution of the traps remains relatively unchanged during exposure to hydrogen. The approximate factor of 2 increase in D_{it} after long exposures to H_2 at room temperature has been seen for all samples studied. For identical MOSFET's which have not been irradiated, however, no increase is observed in D_{it} even after very long hydrogen exposures. This suggests that the radiation has formed defects in the oxide which are able to crack H_2. From these and other studies, it was suggested[17,19,20] that H_2 is cracked in the oxide by the reaction

$$H_2 + D^+ \Longrightarrow HD + H^+$$

where D^+ is a positively charged defect formed by the irradiation. The H^+ formed in this reaction quickly moves to the interface to form an interface state in a process identical to that which has been suggested to occur during irradiation.[21] From the relationship between the number of interface traps formed during irradiation and the number formed during the postirradiation hydrogen exposure, it has been suggested[20,22] that the D^+ cracking sites are created when holes generated during the irradiation knock hydrogen atoms off $O_3 \equiv Si\text{-}H$ or $O_3 \equiv Si\text{-}OH$ defects in the oxide (the $O_3 \equiv$ symbol represents three back bonds to the network oxygen atoms).

D. Permeability determination

Figure 3 shows the increase in I_{cp} as a function of the square root of the hydrogen exposure time t for 4 MOSFET's fabricated on the same chip. Each of the MOSFET's shown had a gate oxide which was grown in dry oxygen to a thickness of 354 Å. The devices were all identical except for their gate length, which varied from 4.0 to 21.3 μm. The devices were irradiated with x rays to a dose of 2 Mrad one day prior to the hydrogen exposure. Forming gas was used as the source of hydrogen.

The linear increase in I_{cp} when plotted as a function of $\sqrt{t}$ suggests that the increase results from the lateral diffusion of the H_2 into the oxide. This conclusion is also supported by the observation from Fig. 3 that the time to reach saturation varies as L_g^2. If the rate of increase in I_{cp} is, in fact, caused by the diffusion of hydrogen into the oxide, then it should be possible to calculate the hydrogen diffusivity by measuring the rate at which I_{cp} increases during the hydrogen exposure. An approximate method for doing this was outlined in a previous paper,[16] and was used to estimate the room temperature permeability of hydrogen in dry thermal oxides. The method described in that paper will be reviewed here. An enhancement of the method will then be presented which allows a more accurate determination of the permeability to be made, and for the diffusivity and solubility to be individually determined.

As pointed out in Sec. II C, the increase in N_{it} results from the cracking of hydrogen molecules at radiation induced cracking sites in the bulk of the oxide. The byproduct of this reaction is H^+, which under positive gate bias drifts to the Si-SiO_2 interface, where it forms interface states. In modeling the diffusion of the H_2 into the oxide, then, it is necessary to include the loss of the H_2 (and the loss of the cracking site) which occurs immediately preceding the formation of the interface trap. If the rate of reaction between the cracking site and the H_2 is very fast compared to the diffusion rate, then the H_2 diffusion can be described by the tarnishing model discussed by Shelby.[23,24] Because of the fast reaction rate, as the hydrogen diffuses into the oxide a sharp boundary forms at a distance X from each side of the gate oxide from which the hydrogen is entering (i.e., from the width of the gate). This is illustrated in Fig. 4. No hydrogen

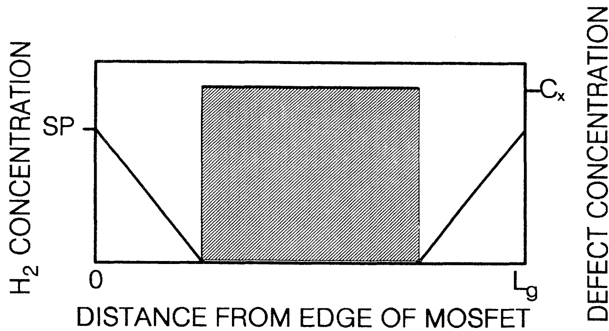

FIG. 4. Concentration of H_2 (triangular regions) and cracking defects (shaded region) in oxide after a time $t < t_{sat}$. At $t=0$ cracking defect concentration was C_x throughout oxide, and H_2 concentration was zero.

has diffused inside this boundary, so the concentration of cracking sites is still C_x in the inner regions of the MOSFET. On the other side of this boundary all cracking sites have been removed. At the outer region of the oxide the concentration of hydrogen is SP, where S is the hydrogen solubility and P is the hydrogen partial pressure. The hydrogen concentration decreases in the outer regions of the oxide to a value of zero at the moving boundary as shown in Fig. 4.

The distance X is given as a function of t by[23–25]

$$X=\left[\frac{2fKPt}{C_x}\right]^{1/2}=\left[\frac{2fSDPt}{C_x}\right]^{1/2} . \tag{2}$$

The factor f in Eq. (2) is a function of SP/C_x, and is described by Booth.[25] Because of its importance in separating S and D from K, f is plotted in Fig. 5. For the samples studied here, SP/C_x ranges from 0.1 to 20, so f ranges from 1 to about 0.2. In deriving Eq. (2) it was assumed that the concentration of cracking sites is initially uniform throughout the oxide. But, as discussed in Refs. 20 and 22, the concentration of cracking sites may depend on the distance from the Si-SiO_2 interface. This does not have a significant effect on the validity of Eq. (2) in modeling the H_2 diffusion, however, since the lateral diffusion distance of the H_2 (2–25 μm) is very large compared to the H_2 hopping distance (a few Å) and the oxide thickness (95–1140 Å). In other words, as the H_2 diffuses along the length of the gate oxide, it uniformly "samples" the entire oxide, so only the average value of C_x perpendicular to the interface is of importance.

The number of cracking sites which have been removed at time t is given by C_x times the volume of oxide which has been cleared of cracking defects, $2XWT$. The removal of each cracking site produces a single H^+ which then quickly moves to the interface where it forms an interface trap. The number of interface traps formed at time t as a result of cracking H_2 is therefore

$$\Delta N_{it}^{*}=WT\sqrt{8fSDPC_x t} . \tag{3}$$

This relationship is valid for $t < t_{sat}$, the time at which the two moving boundaries meet at the center of the oxide. At $t=t_{sat}$ no cracking sites remain, and growth in N_{it} saturates. From Eq. (2)

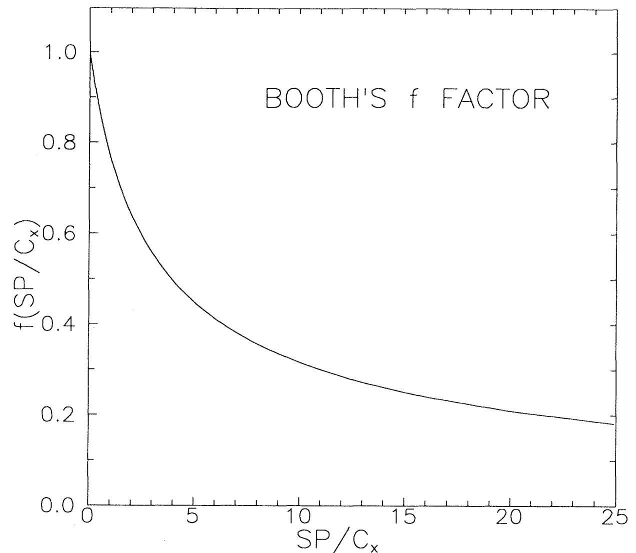

FIG. 5. Booth's f factor as a function of SP/C_x.

$$t_{sat}=\frac{C_x L_g^2}{8fSDP} . \tag{4}$$

Equations (3) and (4) predict that the growth rate of N_{it}^{*} and t_{sat} should both depend on the number of radiation induced cracking sites, C_x, and on the partial pressure of the hydrogen, P. To test these predictions four identical MOSFET's were irradiated to a dose of either 0.1 or 0.5 Mrad, then exposed to either pure hydrogen or forming gas (10.0% hydrogen). The increase in I_{cp} [which is linearly related to the number of interface traps by Eq. (1)] was monitored during the hydrogen exposure. As Fig. 6 shows, the MOSFET's irradiated at the higher doses have more radiation induced cracking sites, and therefore produce more interface traps during hydrogen exposure than MOSFET's irradiated at lower doses. Figure 6 also provides verification of the dependencies on C_x and P predicted by Eqs. (3) and (4). Note, for example, that I_{cp} rises faster when either the hydrogen pressure or radiation dosage is increased, in accordance with Eq. (3), whereas the time required to reach saturation increases when the radiation dosage is increased, or when the partial pressure is decreased, in accordance with Eq. (4).

The validity of the model developed above is also shown by the linear increase in I_{cp} (and therefore N_{it}^{*}) when plotted as a function of $\sqrt{t}$, as shown in Figs. 3 and 6. When MOSFET's which are identical except for their gate lengths are exposed to the same radiation dosage, it is expected that they will all have the same value of C_x. According to Eq. (3) when these MOSFET's are then exposed to hydrogen the rate of increase in N_{it} should be the same for each MOSFET when plotted as a function of $\sqrt{t}$. Figure 3 shows that this is the case.

The curves shown in Figs. 3 and 6 do not pass through the origin as expected from Eq. (3). This is because the MOSFET source and drain regions extend slightly under the gate oxide, as shown in Fig. 1. Since the charge

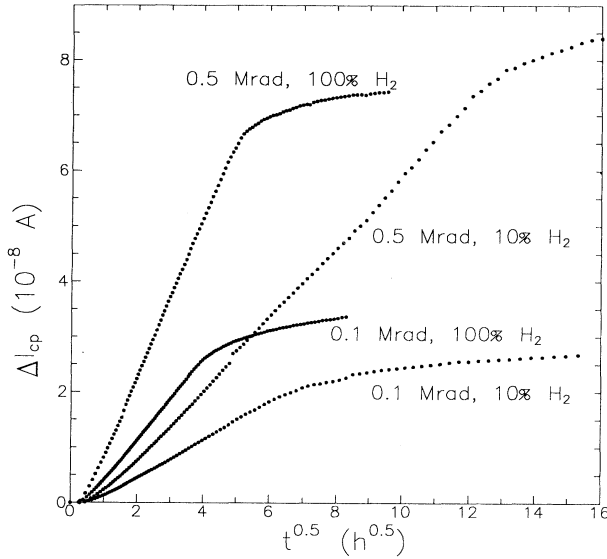

FIG. 6. Increase in charge pumping current (I_{cp}) as a function of square root of time in hours for four identical MOSFET's which were first irradiated with x rays to a dose of either 0.1 or 0.5 Mrad, then exposed to either pure H_2 or to forming gas (10.0% H_2). Gate oxides were all 478-Å-thick pyrogenic oxides grown at 900 °C.

pumping measurements only detect interface traps in the region between the source and drain, the hydrogen must therefore diffuse a short distance into the gate oxide before the resulting increase in the number of interface traps is observed by the charge pumping measurements. In determining the saturation value of I_{cp} this effect can be compensated for by shifting the I_{cp} axis upward slightly so that the curves pass through the origin. The added charge pumping current reflects interface traps formed by the cracking of H_2 in the region of overlap between the oxide and the source and drain.

The number of interface traps, N_{it}^*, shown in Eq. (3) is the number of traps formed in the entire band gap. As discussed in Sec. II B, however, the charge pumping technique only detects those traps in the central 0.5 eV of the gap. From Fig. 2 we can estimate that approximately 40% of the traps are not included in the N_{it} calculated using Eq. (1). We therefore assume that

$$N_{it}^* \simeq 1.4 N_{it} = 1.4 \frac{I_{cp}}{\omega q A} . \tag{5}$$

Errors which might be introduced into the calculation of D, S, and K by inaccuracies of this approximation will be discussed below.

Solving Eq. (3) for SD, we find

$$K \equiv SD = \frac{1}{8fPC_x W^2 T^2} \left[\frac{\delta \Delta N_{it}^*}{\delta \sqrt{t}} \right]^2 , \tag{6}$$

where the term in parentheses is the slope of the ΔN_{it}^* versus $\sqrt{t}$ curve before saturation. To use Eq. (6) we must first determine C_x. Since one interface trap is formed from each cracking defect,

$$C_x = \frac{\Delta N_{it}^*(\text{sat})}{L_g WT} , \tag{7}$$

where $N_{it}^*(\text{sat})$ is the number of interface traps formed at time t_{sat}, and $L_g WT$ is the volume of the gate oxide.

Because f is a function of SP/C_x, S effectively appears on both sides of Eq. (6), and a value of K cannot be obtained from a single set of data. But because f is only weakly dependent on SP/C_x (see Fig. 5), we can obtain an approximate value for K from a single set of data by assuming that either S or D has the same value in these films as in bulk SiO_2. This is the approach which was taken in Ref. 16.

We point out here, however, that it is possible to obtain values for S and D independently, and therefore obtain more accurate values of K by comparing the rate at which I_{cp} increases when identical MOSFET's are irradiated to different doses (so as to change C_x) and/or exposed to different partial pressures of hydrogen. In this way the value of f can be modified and self-consistent values of S and D determined. This is illustrated in Fig. 7, which shows values of K/K_b and D/D_b calculated using Eq. (6) when various values are assumed for S. In these plots $K_b = 1.4 \times 10^7$ cm^{-1}sec^{-1}atm^{-1} and $D_b = 1.4 \times 10^{-11}$ cm^{2}sec^{-1} are the permeability and diffusivity, respectively, of H_2 in bulk SiO_2.[26] The three sets of data converge near an assumed solubility of $0.4 \pm 0.1 \times 10^{18}$ cm^{-3}atm^{-1}, somewhat less than the value 1×10^{18} cm^{-3}atm^{-1} which has been reported for

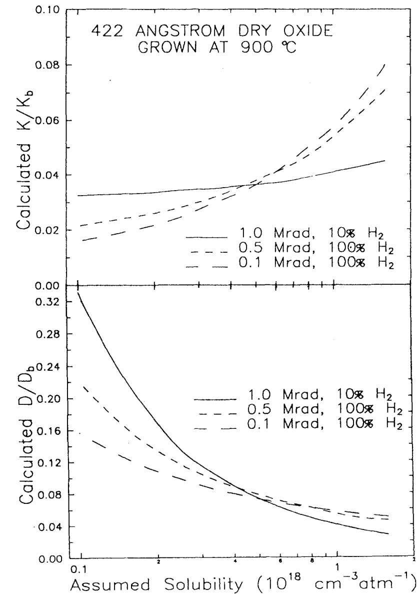

FIG. 7. Method for independent determination of diffusivity and solubility. Top panel shows calculated values for permeability K (normalized to bulk value, K_b) as a function of the assumed value of the solubility. Lower panel shows calculated values of diffusivity D (normalized to bulk value, D_b) as a function of the assumed value of the solubility. Data for three identical MOSFET's with 422-Å-thick oxides are shown. Each MOSFET was irradiated to a different dose and/or exposed to a different H_2 partial pressure.

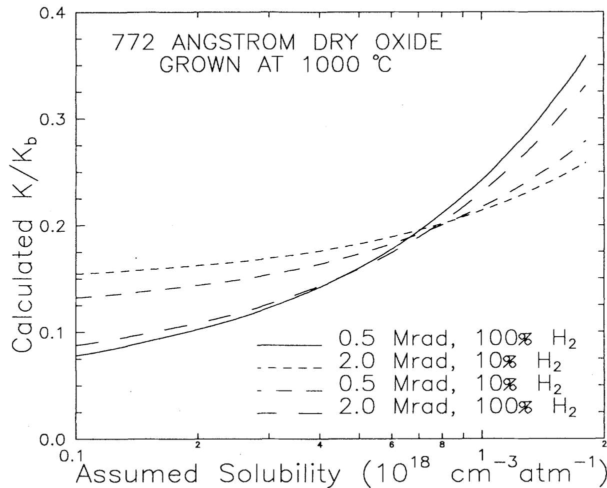

FIG. 8. Data similar to top panel of Fig. 7, but for 772 Å thick oxide grown at 1000 °C.

the hydrogen solubility in bulk SiO_2 at room temperature.[26] Note that the three lines do not cross at a single value of the assumed solubility; this is primarily the result of inaccuracies in the determination of the gate length, but may also reflect experimental problems which will be addressed later. We believe that the results for K have a precision of about 30%, but the values determined for S and D may be precise to only a factor of 2 or worse. Similar data for a 772 Å oxide grown at 1000 °C are shown in Fig. 8.

The impact of using the f factor to determine S and D independently is indicated in Fig. 7. Had it been (incorrectly) assumed, for example, that the solubility was the same in these thermal oxides as in bulk SiO_2, then the calculated value of K would have been erroneously large and the calculated value of D would have been erroneously small. On the other hand, had it been (incorrectly) assumed that the diffusivity was the same in these thermal oxides as in bulk SiO_2, then the calculated values of both K and S would have been erroneously small. The magnitude of the errors would have depended on the radiation dose and partial pressure (through the ratio SP/C_x). Such a determination was reported earlier[16] for dry thermal oxides. In that study a relatively large dosage (1 Mrad) and small hydrogen partial pressure (0.1 atm) were used (corresponding to the data shown by the solid line in Fig. 7), so errors in the reported values of K were relatively small.

III. EXPERIMENTAL RESULTS

The permeability, diffusivity, and solubility of various thicknesses of dry and pyrogenic oxides were determined using the method described above. Our experimentally determined values for K for the pyrogenic oxides grown at 900 °C are shown in Fig. 9.

In view of earlier studies[2,3] discussed in Sec. I which reported the existence of a transition layer near the Si-SiO_2 interface, it seems plausible that the thickness dependence of K shown in Fig. 9 may arise because an

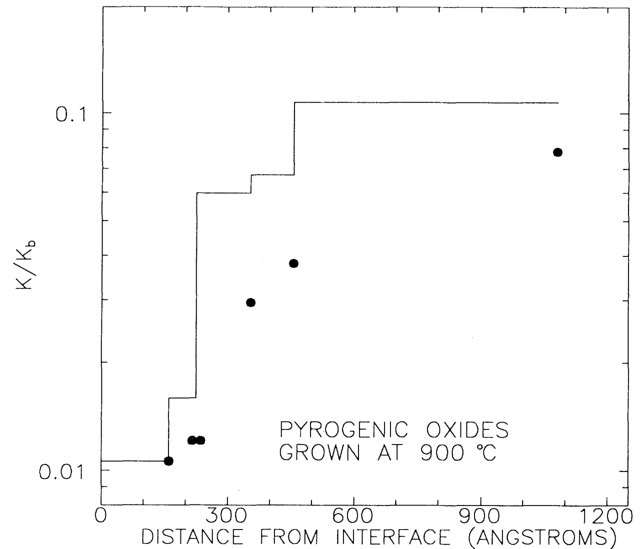

FIG. 9. Experimentally determined values of permeability K (normalized to bulk value, K_b) as a function of oxide thickness for pyrogenic oxides grown at 900 °C. Points are average values over entire oxide thickness, lines are deconvolved values of the average permeability over various ranges of oxide thickness.

average value of K over the entire oxide thickness is determined experimentally. The measured permeability for an oxide of thickness T is

$$K(T) \equiv K_{\text{ave}}(0 \rightarrow T) = \frac{1}{T} \int_0^T K'(x)\,dx \;, \tag{8}$$

where $K'(x)$ is the local permeability at a distance x from the interface. If the transition layer has a very small permeability, then $K_{\text{ave}}(0 \rightarrow T)$ will be smaller than the local permeability of the bulk of the oxide, and $K_{\text{ave}}(0 \rightarrow T)$ will appear to decrease as T is decreased. To determine whether an interfacial layer might be responsible for the apparent gradient in K, we have determined average values of K over smaller segments of the oxide using

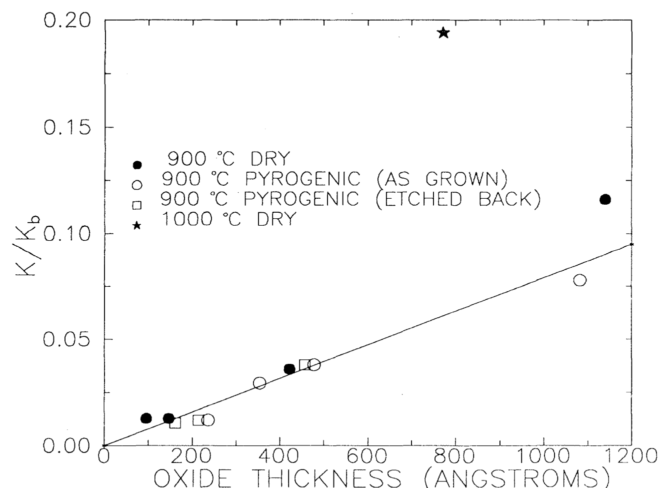

FIG. 10. Experimentally determined values of permeability K (normalized to bulk value, K_b) as a function of oxide thickness.

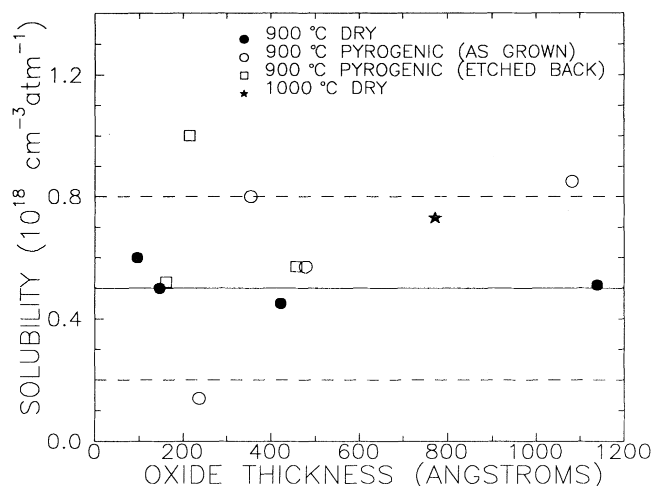

FIG. 11. Experimentally determined values for solubility S as function of oxide thickness.

$$K_{\rm ave}(T_x \rightarrow T) = \frac{T K_{\rm ave}(0 \rightarrow T) - T_x K_{\rm ave}(0 \rightarrow T_x)}{T - T_x} , \quad (9)$$

where T_x is an intermediate oxide thickness. If we assume that the thicker oxides are identical to the thinner oxides, but have an additional layer on top, then we can use Eq. (9) to determine the permeability of the additional layer. Figure 9 shows the results of this deconvolution; the solid horizontal lines are the average permeabilities over segments of the oxide. Had the thickness dependence observed in the measured values of K resulted solely from a low permeability transition layer near the interface, the average values of K in regions beyond the transition layer would have been constant. Figure 9 indicates that this is not the case.

In Fig. 9 the permeability was plotted on a log scale to emphasize the data for the thin oxides. In Fig. 10 the H_2 permeability is plotted on a linear scale. The thickness dependence of the permeabilities for all the oxides grown at 900 °C can be described by the straight line shown. If the measured permeabilities are, in fact, linear with oxide thickness, then the local permeability at any distance from the interface will be twice the permeability measured for an oxide of that thickness. Our experimentally determined values for S are shown in Fig. 11, and display no clear dependence on oxide thickness; for the oxides grown at 900 °C S remains relatively constant at about $5 \pm 3 \times 10^{17}$ cm^{-3} atm^{-1}. These figures also show the results for 772-Å-thick oxides grown in dry oxygen at 1000 °C; these oxides have significantly larger values of K but S is similar to that of the oxides grown at 900 °C.

IV. DISCUSSION

The data shown in Figs. 10 and 11 show several rather surprising results: (i) even the thickest oxides have permeabilities which are much smaller than that of bulk SiO_2, (ii) the oxides have a permeability gradient which extends at least several hundred Å from the interface, (iii) the permeability of oxides etched back to a given thickness is similar to those grown directly to the same thickness, and (iv) higher growth temperature results in higher permeability. These results will be discussed in this section.

Figure 10 indicates that even the thickest 900 °C oxides studied have permeabilities which are an order of magnitude smaller than the permeability of bulk SiO_2. It is well known from ellipsometry studies[27,28] that thermal oxides grown below a certain temperature have larger refractive indexes than bulk SiO_2. This temperature is 1150 °C for dry grown oxides and 1000 °C for wet grown oxides. The increase in refractive index is attributed to densification of the thermal oxide. We propose that the decreased permeability shown in Fig. 10 is also a result of densification.

Shelby[29] studied the diffusivity of helium in densified B_2O_3 glass at 100 °C, and found that the diffusivity varies inversely with glass density. His results are replotted in Fig. 12. We have used spectroscopic ellipsometry to determine the density of a thermal oxide grown under the same conditions as the 1082 Å pyrogenic oxide MOSFET, and have found that this oxide is compacted by about 3.3%. From Fig. 12 it is seen that this densification of B_2O_3 would reduce the diffusivity of He by about a factor of 2.5. Shelby's results also show that the solubility is reduced by the densification, so that the total reduction in permeability would be about a factor of 5, similar to the factor of 12 that we observe for the decrease in the room temperature diffusivity of H_2 through our thick SiO_2 oxides. His observation that the solubility is lower in densified glass is also in agreement with our results (see Fig. 11), if our oxides are densified.

The dependence of permeability on glass densification has also been suggested from several studies[30–32] which used less direct methods. In these studies thermal oxides were grown at various temperatures (and in some cases further annealed at another temperature), then reoxidized. The oxide density was inferred from the refractive index of the oxide before the reoxidation, and the per-

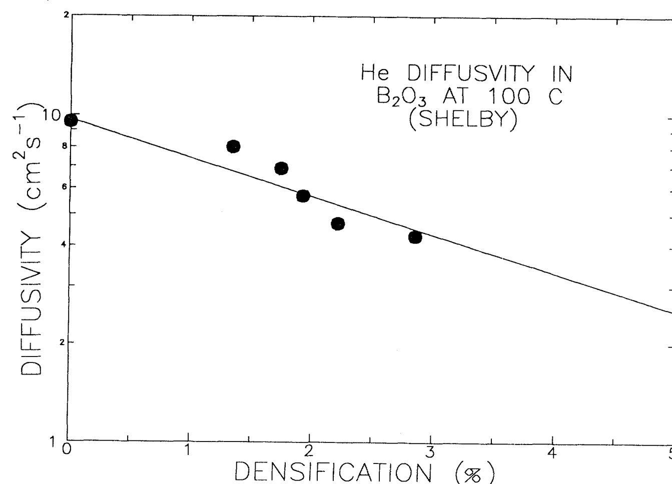

FIG. 12. Data of Shelby (Ref. 29) for the diffusivity of He in B_2O_3 glass at 100 °C as a function of glass densification.

meability of the oxide was calculated from the increase in the oxide thickness which occurred during the reoxidation. Some of these studies[31,32] also indicated an exponential dependence of the O_2 permeability on the glass density. Tanaguchi *et al.*[32] state that a 3% compaction results in an order of magnitude decrease in the O_2 permeability, very close to our value for the decrease in the H_2 permeability at room temperature.

Since the lower permeability of the thick oxides can be attributed to their increased density, we suggest that the decrease in the permeability as the oxide thickness decreases is a reflection of a gradient in the oxide density. From Fig. 12 and Ref. 32 permeability appears to vary exponentially with density. The linear dependence of K on oxide thickness shown in Fig. 10 then suggests that from 160 to 1200 Å the oxide density ρ varies as

$$\rho-\rho_0 \propto -\ln(x) , \tag{10}$$

where x is the distance from the Si-SiO_2 interface. Since for the 1082 Å pyrogenic oxide a 3.3% compaction results in a factor of 12 decrease in the permeability, the factor of 100 decrease in the permeability we observe for oxides approximately 160 Å thick can be explained by assuming a 6% average densification for these oxides.

Direct verification of a densification of this magnitude is extremely difficult. Although, as discussed by Kalnitsky *et al.*,[4] random errors in even the most precise ellipsometers make the determination of the density of thin oxides very difficult, most ellipsometric studies indicate that the index of refraction increases as an oxide is thinned by etching (see, for example, Fig. 7 of Ref. 4). Aspnes *et al.*[2] attributed this to the presence of an interface. They determined that the interfacial layer had the least influence on their data for oxides near 1400 Å in thickness, so in their determination of the thickness and stoichiometry of the interfacial layer they *assumed* that oxides of all thicknesses had the same density as their 1400-Å-thick oxide. Kalnitsky *et al.*[4] reported that they could explain their (single wavelength) ellipsometric etchback data as a result of a transition layer with a graded index of refraction. In this model the index corresponded to a densification of the oxide greatly exceeding 10% at distances within 40 Å of the interface. At distances greater than 60 Å from the interface, their model includes no oxide densification.

The above paragraph illustrates the difficulty in accurately determining the oxide density using ellipsometry. It is clear that there is some densification of the oxide, but the spatial distribution of the densification is unknown. The rather small gradient in density (increasing from 3.3% to 6% as the distance is decreased from 1100 to 160 Å) proposed above to explain our H_2 permeability results does not seem to conflict with any known ellipsometry data.

A number of models have been proposed to explain why thermally grown SiO_2 films have larger refractive indexes than bulk SiO_2. Most of these models attribute the increase to an increased oxide density which results from strain at the interface. This strain is believed to arise from the inability of the oxide to totally accommodate the increase in molar volume as new oxide grows at the Si/SiO_2 interface. Measurements by Taft[28] indicate that the refractive index depends on growth temperature, suggesting that during growth the oxide undergoes viscous flow[33] or a similar process[34] to relax the strain. These results are in agreement with direct measurements of the density of oxides by Irene *et al.*[35] who reported that oxides grown at 800 °C have larger densities than oxides grown at 1000 °C, presumably because the oxide grown at the higher temperature was able to relax during growth.

Fitch *et al.*[36] have measured the total stress in oxides of various thickness grown at 700 °C and 1000 °C, and correlated these results to the strain as determined by their infrared absorbance measurements of the bond-stretching frequencies. Their results indicate that the magnitude of the strain depends on the oxide thickness and growth temperature. For oxides grown at low temperatures, the strain decreases very slowly with increasing oxide thickness, whereas for oxides grown at higher temperatures (above 1000 °C) the decrease is much more rapid. Even for oxides grown at 1000 °C, however, oxides several hundred Å thick show significant strain. Their results are in good qualitative agreement with the density gradient required to explain our permeability measurements.

Mrstik *et al.*[37] reported that a 1150-Å-thick oxide grown in dry oxygen at 1000 °C was densified by 1.91%, considerably less than the 3.3% densification of the 1082 Å thick oxide grown at 900 °C used in this work. From the exponential dependence of permeability on oxide density, this would imply that the 1000 °C oxide should have a permeability about three times larger than an oxide of similar thickness grown at 900 °C. Figure 10 shows that this prediction is accurate. Since Shelby's results[29] indicate that solubility is inversely related to density, the 1000 °C oxide should also have a solubility closer to the bulk value (1×10^{18} cm^{-3} atm^{-1}) than do the 900 °C oxides. Figure 11 indicates that this is also in agreement with our results.

The dependence of the permeability on oxide thickness reported here has important implications on the oxide growth kinetics. The growth rate of SiO_2 on Si was modeled by Deal and Grove.[7] In their model the growth rate is determined by the rate at which the oxidant can be consumed at the Si/SiO_2 interface and the rate at which it can be transported through the oxide. The inverse growth rate is therefore

$$\frac{dt}{dx}=\frac{1}{k_l}+\frac{2x}{k_p} , \tag{11}$$

where t is the oxidation time, x is the oxide thickness, k_l is the linear rate constant, which is related to the surface reaction rate, and k_p is the parabolic rate constant, which is proportional to the permeability of the oxidant in the oxide.

The model is very successful in describing the growth rate of wet oxides, in which the oxidizing species are hydroxyl groups. It is well known, however, that when the oxidant is dry oxygen, the oxides grow faster than predicted by the model during the early stages of growth.

This "fast growth" regime has been the subject of numerous papers (see, for example, Ref. 38). In one of these papers Revesz *et al.*[39] pointed out that the anomaly actually exists at all thicknesses, and attributed it to a dependence of the oxygen diffusivity on the oxide thickness. Thus, whereas k_p in the Deal and Grove model is constant, Revesz *et al.* suggested that k_p increases linearly as the oxide thickness increases, i.e.,

$$k_p = k_t + x k_0 \ . \quad (12)$$

This model produced excellent agreement with measured growth rates.

The thickness dependence of k_p determined by Revesz *et al.* is shown in Fig. 13 for oxides grown at 870 °C and 1000 °C. At low growth temperature, the thickness dependence of k_p is similar to the dependence shown in Fig. 10 for the room temperature permeability of hydrogen in SiO_2. This is additional support for our hypothesis that our observed dependence of hydrogen permeability on oxide thickness is due to a gradient in the oxide density, since this gradient would also be expected to modify the oxygen diffusivity during oxide growth. Since water diffuses through the oxide by breaking and reforming bonds, however, it would be less sensitive to density changes, so no "fast growth" regime would be expected for pyrogenic or wet oxidation.

Landsberger and Tiller[40] have studied the density relaxation which occurs when dry oxides grown at 800 °C are annealed in inert gas at temperatures from 800 °C to 1100 °C. They find that after growth the oxide is densified by about 3%, but that during the anneal the density approaches that of undensified SiO_2, the rate of approach being dependent on anneal temperature. If the oxide relaxed by Newtonian flow, the density would decrease exponentially with anneal time, much faster than observed. Rafferty *et al.*[41] note that because of the high stress the relaxation must be modeled using non-Newtonian flow to include the effect of stress on the oxide viscosity. Their results are in excellent agreement with

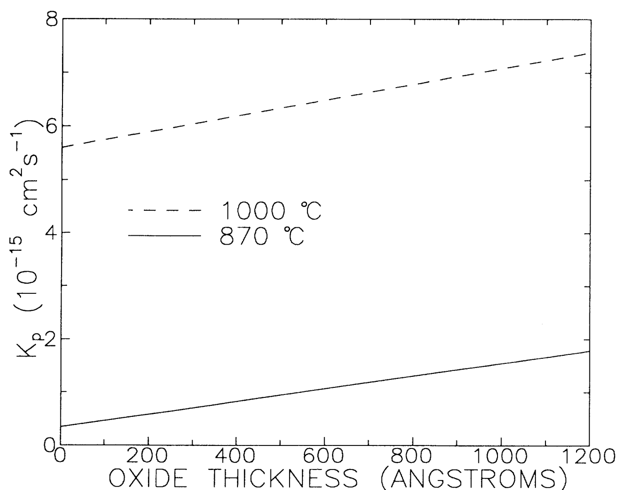

FIG. 13. Thickness dependence of parabolic rate constant determined by Revesz *et al.* (Ref. 39) to describe growth of oxides on Si(100) substrates at 870 °C and 1000 °C.

the experimental data of Landsberger and Tiller, and indicate that at times greater than a few hundred seconds, the density decreases logarithmically with anneal time.

If we assume that the same relaxation is occurring *during* growth as during the inert gas anneal, then the oxide away from the Si-SiO_2 interface must have a lower density than the oxide near the interface because it has had a longer time to relax. According to Eq. (11) for relatively thick oxides, the time to grow an oxide of thickness x varies as x^2. Since Rafferty *et al.* found that the density decreases logarithmically with anneal time, their results suggest that the density should also decrease logarithmically with distance from the Si-SiO_2 interface. This is in agreement with our measurements, as we discussed in deriving Eq. (10).

Although the density gradient implied by our permeability measurements is in general agreement with predictions of Refs. 40 and 41, two aspects of our data need further study. First, Fig. 10 indicates that the dry oxides have nearly identical permeabilities as pyrogenic oxides of similar thickness. This is hard to understand in terms of viscoelastic relaxation because the wet oxides have much smaller viscosities than dry oxides.[42] Although this is compensated for somewhat by their much higher growth rates, it is difficult to accept the similarity in density gradients as being coincidental. Second, Fig. 10 indicates that pyrogenic oxides which were first grown to a thickness of 1082 Å, then etched back to their final thickness (457 Å or 214 Å), have nearly the same permeabilities as oxides grown directly to a similar final thickness. Since the etched oxides have had a longer time to relax, the results of Ref. 41 would suggest that they should have smaller densities and therefore higher permeabilities. Both of these observations suggest that an additional mechanism may be responsible for the relaxation. One possibility is that the oxide structure retains some memory of the epitaxial structure of the interface. Borie *et al.*,[43] for example, report that for the formation of (crystalline) Cu_2O films on Cu crystals the epitaxy significantly affects the strain relaxation throughout the film.

V. SUMMARY

We have described a method for measuring the room temperature permeability of H_2 in thermal oxides on Si substrates, and for determining the solubility and diffusivity independently. The technique is based on the observation that interface traps are formed when an irradiated MOSFET is exposed to hydrogen. The technique requires that certain assumptions be made about the physical processes by which the interface traps are formed. The consequences of these assumptions are examined in detail in the Appendix.

We have used the method to determine the dependence of permeability on oxide thickness. Permeability is extremely sensitive to density, so these measurements provide an excellent probe of the oxide density. Our results indicate the presence of a density gradient in the oxide which extends at least several hundred Å from the interface. These results are in agreement with earlier studies

using infrared techniques, with studies of the oxide growth rate, and with studies of the density relaxation which occurs during annealing in an inert gas.

ACKNOWLEDGMENTS

The authors wish to thank N. S. Saks for providing the MOSFET's used in this study and R. K. Lawrence for irradiating the samples. Special thanks are also due R. W. Rendell for stimulating discussions throughout the work.

APPENDIX: DISCUSSION OF POSSIBLE SOURCES OF ERROR

Because the method used in this study for the measurement of permeability is new, this appendix will carefully examine various aspects of the experimental procedure and of the implicit assumptions made in deducing K from the experimental data.

1. Errors in calculating N_{it}^*

The primary experimental measurement is the charge pumping current, I_{cp}, from which N_{it} can be calculated. But in converting N_{it} to N_{it}^*, for use in Eq. (6) some estimate of the number of interface traps outside the range probed by the charge pumping measurements must be made. From Fig. 2 it appears that D_{it} is small near the band edges, so our factor of 1.4 [used in Eq. (5)] in the conversion of N_{it} to N_{it}^* seems reasonable. It is possible, however, that D_{it} may be large outside the range shown in Fig. 2. The effect of miscounting the number of interface traps can be examined by using Eq. (6) to write an expression for D:

$$D=\frac{1}{8Sf\left[\dfrac{SP}{C_x}\right]PC_xW^2T^2}\left[\frac{\delta\Delta N_{it}^*}{\delta\sqrt{t}}\right]^2 . \tag{A1}$$

If the measured number of traps, N_{it}^m, is related to the actual number by $N_{it}^*=A_0N_{it}^m$, then $C_x=A_0C_x^m$, where C_x^m is the measured concentration of radiation induced defects. In terms of the measured values, then, Eq. (A1) may be rewritten as

$$D=\frac{1}{8\dfrac{S}{A_0}f\left[\dfrac{SP}{A_0C_x^m}\right]PC_x^mW^2T^2}\left[\frac{\delta\Delta N_{it}^m}{\delta\sqrt{t}}\right]^2 . \tag{A2}$$

Equation (A2) is identical to Eq. (A1) if the actual solubility $S=A_0S^m$, where S^m is the solubility determined from the experimental data using Eq. (A1). Errors in counting the number of interface traps will therefore not affect the experimentally determined values of D, but will affect the value determined for S. From Fig. 2 it is clear that we cannot be significantly overestimating N_{it}^*, but we might be underestimating N_{it}^* if a large number of interface traps exists beyond the range probed by the charge pumping measurements. It is therefore more likely that our value for S is too small than too large. But since our value is in reasonable agreement with the value reported as characteristic of bulk SiO_2, we do not believe the error is large. In fact, the close agreement can be taken as evidence that there are few interface traps near or beyond the band edge. Any error in S would also affect the calculated value of K by the same factor. Our observation of a gradient in K would not be affected, however, since A_0 should be independent of thickness.

2. Adsorption/absorption of H_2 at the substrate or polysilicon interface

In modeling the diffusion process, we have assumed that the only loss of H_2 occurs as a result of reaction with the cracking sites, so that an interface trap is formed for each hydrogen molecule which is lost. It is possible, however, that H_2 is also lost through adsorption or absorption at either of the interfaces sandwiching the oxide. Since this would have a larger effect in decreasing the apparent H_2 diffusivity in thin films than in thick films, it could provide an explanation for the apparent gradient in the permeability.

If we assume that the interfaces adsorb H_2, then we can include this effect by replacing C_x in Eq. (2) by

$$C_x\rightarrow C_b+\frac{C_s}{T} , \tag{A3}$$

where C_b is the bulk concentration of radiation induced cracking sites, C_s is the surface concentration of H_2 adsorption sites, and T is the oxide thickness. Equation (4) for the saturation time can therefore be written as

$$t_{sat}=\frac{(TC_b+C_s)L_g^2}{8fPSDT} . \tag{A4}$$

If $C_s \gg TC_b$, Eq. (A2) might predict a thickness dependence similar to that observed. We can rule this out, however, since there would be no dose dependence of t_{sat}; Fig. 6 indicates that there is a dose dependence of t_{sat} and that it is given very well by Eq. (4). Such a modification in C_x would also shift the curves in Fig. 7 so that the curves would no longer intersect near a common point.

3. Errors in calculating C_x: Amphoteric interface traps

If the interface traps are amphoteric, then each hydrogen formed by the cracking of H_2 at the radiation induced cracking sites will form two interface traps rather than just one as has been assumed. As pointed out in Ref. 17, there is some indication that between 1 and 2 interface traps are formed from trapped charge in the oxide (N_{ot}) removed during the hydrogen exposure. The data (and the assumptions made in the calculation of N_{ot}), however, are not accurate enough to determine this ratio reliably. If the interface traps are amphoteric the actual value of C_x will be half as large as we have previously assumed. The result of this on our determination of S, D, and K for one of the oxides is shown in Fig. 14. S is now found to be 2×10^{17} $cm^{-3}\,atm^{-1}$, half as large as before, and D/D_b is found to be 0.35, four times as large as before. K is therefore increased by a factor of 2. These changes in S, D, and K can be understood by examining

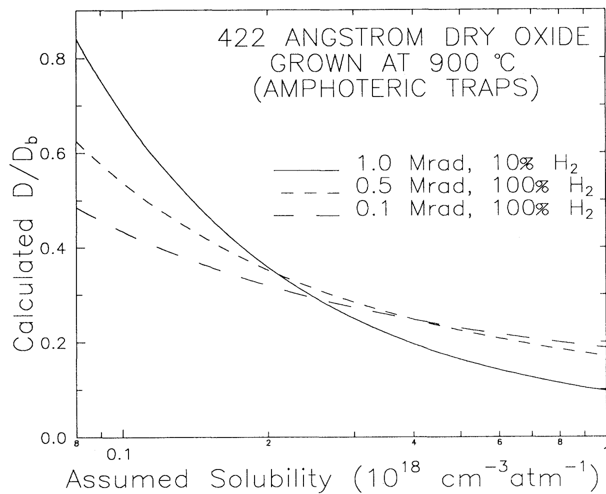

FIG. 14. Same as Fig. 7, but permeability is calculated by assuming that two interface traps are formed from each H_2 molecule which is cracked, rather than just one.

Eq. (6): if C_x is reduced by a factor of 2, the f factor will remain the same if S is also reduced by a factor of 2. D will therefore be increased by a factor of 4, and K will be increased by a factor of 2. Although the values determined for K may be in error by a factor of 2, the gradient in K shown in Fig. 9 will not be unaffected.

4. Errors in calculating C_x: Effects of atomic hydrogen

During the permeability measurements the gate is maintained at a positive bias so that all H^+ formed will drift to the interface, where it can form interface traps. But as seen in Fig. 6 of Ref. 17, some interface traps are also formed when the gate bias is negative. Typically the number of traps formed with negative bias is between 25% and 50% of the number formed with a positive gate bias. The formation of interface traps under negative gate bias suggests that either (i) some of the H^+ which is formed near the interface is drifting against the field, or (ii) that the cracking reaction produces some atomic hydrogen, H_0, which may also form interface traps.

If some H_0 is, in fact, being formed, then our determination of K may be in error if all the H_0 formed does not produce interface traps, since the amount of H_2 consumed will not be properly calculated. Although most of the H_0 striking the Si/SiO_2 interface probably will form an interface trap, and therefore have no effect on our calculations, H_0 may also be lost through several other mechanisms, including the following.

(i) Absorption at SiO_2/poly Si or SiO_2/Si interface. It is known[44] that H_0 formed in an rf plasma can be absorbed into Si substrates. Preliminary measurements by Buchanan,[45] however, have indicated that during the postirradiation hydrogen exposure the amount of H_0 absorbed by the substrate is probably only 1–10% of the amount of H_2 cracked by the positive charge.

(ii) Dimerization. It is possible that the H_0 will dimerize to form H_2 rather than an interface trap. Thus two cracking defects will be removed, but only one H_2 on balance will be consumed, so that C_x will be inaccurately determined. The concentration of H_0 formed during the hydrogen exposure, however, is very small so dimerization is unlikely. Note, however, that during irradiation the concentration of H_0 is much larger, and dimerization is the primary mechanism by which H_0 is consumed.[20,22]

5. By-product of interfacial reactions

We have so far not discussed the reaction at the interface by which an interface trap is formed by the H^+ (or H_0). The interface traps are presumably some variation of the P_b center, a Si atom with three back bonds to Si substrate atoms and a dangling bond. There is some evidence[46,47] that the P_b centers at the SiO_2-Si(111) interface are passivated with hydrogen atoms. The probable reaction at the interface by which the interface trap is formed during postirradiation hydrogen exposure would then be

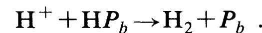

$$H^+ + HP_b \rightarrow H_2 + P_b \ .$$

But if H_2 is formed at the interface, then there will be no net consumption of the H_2 in the oxide, and the tarnishing model used to derive Eq. (2) will not be appropriate. The success of the tarnishing model (with H_2 consumption) in explaining the observed dependence of the rate of N_{it} formation on gate length, defect concentration, and partial pressure leads us to suggest that the above reaction does not occur. Rather, we suggest that the P_b centers are passivated not by hydrogen but perhaps by hydroxyl groups, OH, so that H_2O rather than H_2 is formed when the passivating species is removed by the H^+. A similar problem with reaction (b) was discussed previously.[20] This issue is discussed further in Ref. 48.

6. Reaction rates

In extracting the permeability from our experimental data we have used the tarnishing model for simplicity. The tarnishing model is an accurate solution of the problem of diffusion with consumption only in the limit in which the reaction rate is very fast compared to the diffusion rate, so that a sharp boundary forms at which the density of cracking sites decreases from C_x to zero. Physically, however, the reaction rate is not infinite, so we must verify that it is large enough to ensure the validity of the tarnishing model.

From bimolecular reaction rate theory[49,50] the maximum reaction rate, k, is related to the diffusivity by

$$k = 2\pi\rho D \ , \tag{A5}$$

where ρ is the equivalent reaction radius. Typical reaction radii are usually taken to be about 5 Å. For the 354 Å thick oxide shown in Fig. 3, for which $D/D_b = 0.038$, then, $k = 3.3 \times 10^{19}$ $cm^3 sec^{-1}$. We have numerically solved the differential equation describing the diffusion of hydrogen with consumptive reaction at the cracking site defects and have found that for the case shown in Fig. 3, this value of k leads to a transition region about 0.2 μm wide in which the concentration of the cracking defect goes to zero. This distance is small compared to our shortest device lengths, so the tarnishing model can be

safely used. For reaction rates 100 times smaller than this the transition layer is about 2 μm wide, and a small amount of curvature in $N_{it}(\sqrt{t})$ is observed near $t=0$ and $t=t_{\mathrm{sat}}$.

7. Effect of poor saturation

Figures 3 and 6 indicate that after the rise in $N_{it}(\sqrt{t})$ [or $I_{cp}(\sqrt{t})$] breaks away from the linear portion it does not abruptly saturate as predicted by the tarnishing model. This is seen in all the oxides studied, but is smallest in the hydrogenated oxide, shown in Fig. 6. To understand this we have used numerical simulation to study the H_2 movement through the oxide for conditions more general than those applicable to the tarnishing model.

Attempts to explain the curvature in the N_{it} vs $\sqrt{t}$ plots at long times as the result of a slow reaction rate were found to result in a large curvature at short times as well (as discussed in the Appendix, part 6), contrary to our experimental observations. The reaction rate required to fit the experimental data was found to depend on gate length, also indicating that a slow reaction rate was not responsible for the observed behavior.

We also examined the possibility that two reaction sites are responsible for cracking the H_2, one with a fast reaction rate and one with a smaller reaction rate. This was also found to be incapable of explaining the shape of the curves for all gate lengths.

At least two possibilities remain. The absence of saturation could indicate the presence of cracking sites having a variety of reaction rates. This is certainly a possibility in an amorphous material, since the local geometry might be expected to affect the reaction rate of the cracking site. Another possibility is that the additional N_{it} results from the slow diffusion of the by-products of the interfacial reaction (see the Appendix, part 5) away from the interface.

In extracting S, D, and K from the experimental data no attempt was made to consider the effect of the other mechanism(s) of N_{it} growth; the break point from the linear portion of the curve was used to determine C_x. This is not expected to lead to significant errors in the values deduced for these parameters; without these additional cracking sites the value determined for C_x would have been slightly (about 10%) smaller, but the slope of the ΔI_{cp} vs $\sqrt{t}$ curve also would have been slightly smaller so that, according to Eq. (6), the errors are largely canceled out.

---

[1]S. T. Pantelides and M. Long, in *The Physics of SiO_2 and its Interfaces,* edited by S. T. Pantelides (Pergamon, New York, 1978), p. 333.

[2]D. E. Aspnes and J. B. Theeten, J. Electrochem. Soc. **127**, 1359 (1980).

[3]F. J. Grunthaner and P. J. Grunthaner, Mater. Sci. Rep. **1**, 3 (1986).

[4]A. Kalnitsky, S. P. Tay, J. P. Ellel, S. Chongsawangirod, J. W. Andrews, and E. A. Irene, J. Electrochem. Soc. **137**, 234 (1990).

[5]E. A. Taft, J. Electrochem. Soc. **126**, 131 (1979).

[6]J. E. Shelby, Treatise Mater. Sci. Tech. **17**, 1 (1979).

[7]B. E. Deal and A. S. Grove, J. Appl. Phys. **36**, 3770 (1965).

[8]A. J. Moulson and J. P. Roberts, Trans. Faraday Soc. **57**, 1208 (1961).

[9]F. J. Norton, Nature **171**, 704 (1961).

[10]G. Schols and H. E. Maes, in *Silicon Nitride Thin Insulating Films,* edited by V. J. Kapoor and H. J. Stein (The Electrochemical Society Softbound Proceedings Series, Pennington, NJ, 1983), p. 94.

[11]B. J. Fishbein, J. T. Watt, and J. D. Plummer, J. Electrochem. Soc. **134**, 674 (1987).

[12]R. W. Lee, R. C. Frank, and D. E. Swets, J. Chem. Phys. **36**, 1062 (1961).

[13]W. G. Perkins and D. R. Begeal, J. Chem. Phys. **54**, 1683 (1971).

[14]J. E. Shelby, J. Appl. Phys. **48**, 3387 (1977).

[15]K. L. Brower, Appl. Phys. Lett. **53**, 508 (1988).

[16]B. J. Mrstik, P. J. McMarr, N. S. Saks, R. W. Rendell, and R. B. Klein, Phys. Rev. B **47**, 4115 (1993).

[17]B. J. Mrstik, J. Electron. Mater. **20**, 627 (1991).

[18]G. Groesenecken, H. E. Maes, N. Beltran, and R. F. Keersmaecker, IEEE Trans. Elec. Dev. **ED-31**, 42 (1984).

[19]R. E. Stahlbush, B. J. Mrstik, and R. K. Lawrence, IEEE Trans. Nucl. Sci. **NS-37**, 1641 (1990).

[20]B. J. Mrstik and R. W. Rendell, IEEE Trans. Nucl. Sci. **NS-38**, 1101 (1991).

[21]F. B. McLean, IEEE Trans. Nucl. Sci. **NS-27**, 1651 (1980).

[22]B. J. Mrstik and R. W. Rendell, Appl. Phys. Lett. **59**, 3012 (1991).

[23]J. E. Shelby, J. Appl. Phys. **51**, 2589 (1980).

[24]J. E. Shelby, J. Am. Ceram. Soc. **67**, C-93 (1984).

[25]F. Booth, Trans. Faraday Soc. **44**, 796 (1948).

[26]J. E. Shelby, J. Appl. Phys. **48**, 3387 (1977).

[27]E. A. Taft, J. Electrochem. Soc. **125**, 968 (1978).

[28]E. A. Taft, J. Electrochem. Soc. **127**, 993 (1980).

[29]J. E. Shelby, J. Non-Cryst. Solids **14**, 288 (1974).

[30]E. A. Taft, J. Electrochem. Soc. **132**, 2486 (1985).

[31]L. M. Landsberger and W. A. Tiller, in *The Physics and Chemistry of SiO_2 and the Si-SiO_2 Interface,* edited by C. R. Helms and B. E. Deal (Plenum, New York, 1988), p. 159.

[32]K. Taniguchi, M. Tanaka, C. Hamaguchi, and K. Imai, J. Appl. Phys. **67**, 2195 (1990).

[33]E. A. Irene, G. Tierney, and J. Angilello, J. Electrochem. Soc. **129**, 2594 (1983).

[34]B. J. Mrstik, A. G. Revesz, M. Ancona, and H. L. Hughes, J. Electrochem. Soc. **134**, 2020 (1987).

[35]E. A. Irene, D. W. Dong, and R. J. Zeto, J. Electrochem. Soc. **127**, 396 (1980).

[36]J. T. Fitch, G. Lucovsky, E. Kobeda, and E. A. Irene, J. Vac. Sci. Technol. **B7**, 153 (1989).

[37]B. J. Mrstik, P. J. McMarr, J. R. Blanco, and J. M. Bennett, J. Electrochem. Soc. **138**, 1770 (1991).

[38]*The Physics and Chemistry of SiO_2 and the Si-SiO_2 Interface* (Ref. 31), pp. 1–102.

[39]A. G. Revesz, B. J. Mrstik, H. L. Hughes, and D. McCarthy, J. Electrochem. Soc. **133**, 586 (1986).

[40]L. M. Landsberger and W. A. Tiller, Appl. Phys. Lett. **51**, 1461 (1987).

[41]C. S. Rafferty, L. M. Landsberger, R. W. Dutton, and W. A. Tiller, Appl. Phys. Lett. **54**, 151 (1989).

[42]G. Hetherington, K. H. Jack, and J. C. Kennedy, Phys. Chem.

Glasses **5**, 130 (1964).
[43]B. Borie, C. J. Sparks, Jr., and J. V. Cathcart, Acta Metall. **10**, 691 (1962).
[44]J. I. Pankove and N. M. Johnson, Semicond. Semimet. **34**, 1 (1991). Also see related articles in same volume.
[45]D. A. Buchanan (private communication).
[46]K. L. Brower, Phys. Rev. B **38**, 9657 (1988).
[47]K. L. Brower, Phys. Rev. B **42**, 3444 (1990).
[48]B. J. Mrstik (unpublished).
[49]T. R. Waite, Phys. Rev. **107**, 463 (1957).
[50]R. M. Noyes, Prog. React. Kin. **1**, 129 (1961).